A procedure to determine the radiation isocenter size in a linear accelerator

A. González, I. Castro, and J. A. Martnez

A procedure to determine the radiation isocenter size in a linear accelerator

A. González,[a] I. Castro, and J. A. Martínez
Servicio de Radiofísica y Protección Radiológica, Hospital Universitario Virgen de la Arrixaca,
Ctra. Madrid-Cartagena S/N, El Palmar (Murcia) E-30120, Spain

Measurement of radiation isocenter is a fundamental part of commissioning and quality assurance (QA) for a linear accelerator (linac). In this work we present an automated procedure for the analysis of the stars-shots employed in the radiation isocenter determination. Once the star-shot film has been developed and digitized, the resulting image is analyzed by scanning concentric circles centered around the intersection of the lasers that had been previously marked on the film. The center and the radius of the minimum circle intersecting the central rays are determined with an accuracy and precision better than 1% of the pixel size. The procedure is applied to the position and size determination of the radiation isocenter by means of the analysis of star-shots, placed in different planes with respect to the gantry, couch and collimator rotation axes. © *2004 American Association of Physicists in Medicine.* [DOI: 10.1118/1.1755491]

I. INTRODUCTION

Quality assurance is a fundamental concern in all the processes involved in external radiation therapy with a linear accelerator. In particular, the technical aspects of QA have been the object of several protocols, codes of practice and recommendations.[1,2] A central concern is always the size and position determination of the isocenter, because the isocenter is the primary reference location of external beam radiotherapy.

The ideal isocenter of the machine is defined as a point at which the axis of rotation of the collimator intersects the axis of rotation of the gantry,[3] or more generally, the point at which the axes of rotation of the gantry, collimator and couch intersect.[1] However, the gantry frame tends to flex during rotation which causes the collimator axis to miss the gantry axis. Rotation about the couch and collimator axes may increase the size of the minimum sphere containing the isocenter locus.

Several methods have been described for the optical,[4–6] mechanical[6–9] and radiation[4,10–12] isocenter determination. In particular, when the radiation isocenter is measured by means of star-shots, the tests are generally executed semi-independently for the accelerator components that can rotate[1] (gantry, couch and collimator). In this approach, the trajectory of the radiation field at varying angles is captured on a radiographic film. Then the central rays of the beams are delineated and analyzed to verify that their intersections are contained within the tolerance range.[4] This procedure is considered sufficiently accurate to determine if the performance of the machine meets currently accepted tolerances. However it is time consuming and labor intensive because working with such small spatial dimensions is difficult. On the other hand, the use of IMRT and micro multileaf collimators suggest that more sophisticated techniques would be needed to accurately characterize the linac isocenter.

In this paper we present a procedure for the determination of the radiation isocenter size taking into account its dependence on gantry, couch and collimator rotations and its three-dimensional (3-D) nature. For present purposes, the isocenter position and size are defined, respectively, as the center and radius of the smallest sphere that intersects all the central rays of a series of beams, each directed from a different combination of gantry, couch and collimator angles. A dedicated software was developed to analyze the two-dimensional (2-D) star-shot images with the aim of substituting those parts of the traditional procedure that most likely introduce errors. In order to evaluate the automated analysis implemented, a test was performed using drawn star-shots of exactly known central rays position. Finally, the procedure was applied to the radiation isocenter position and size determination of a linac.

II. MATERIALS AND METHODS

An Elekta Precise (Elekta Oncology Systems Ltd., Crawley, West Sussex, UK) linear accelerator with 4 MV, 6 MV and 15 MV x-ray energies equipped with a multileaf collimator (MLC) was used. The incident photon energy selected was 6 MV for a collimator setting of 0.5×20 cm^2. The narrow dimension was collimated by the conventional (no MLC) jaws.

Films X-Omat V (Eastman Kodak Co., Rochester, NY) were used to obtain 2-D star-shots. Each film was taped to a PMMA block of $20 \times 20 \times 3$ cm^3. The assembly was placed on the accelerator couch "tennis racket" and the film was centered at the laser intersection, previously adjusted to the mechanical isocenter.

For digitizing the films a MicroTek ScanMaker 9600 XL CCD (Microtek International Inc., Husinchu, Taiwan) scanner was used. The output images resulting from digitization were stored in an 8 bits bitmap (BMP) file format. The image acquisition was carried out without the use of filters and with $\gamma = 1$. In these conditions, reading is linear with film transmission in the OD interval from 0.14 to 1.86 (linear correla-
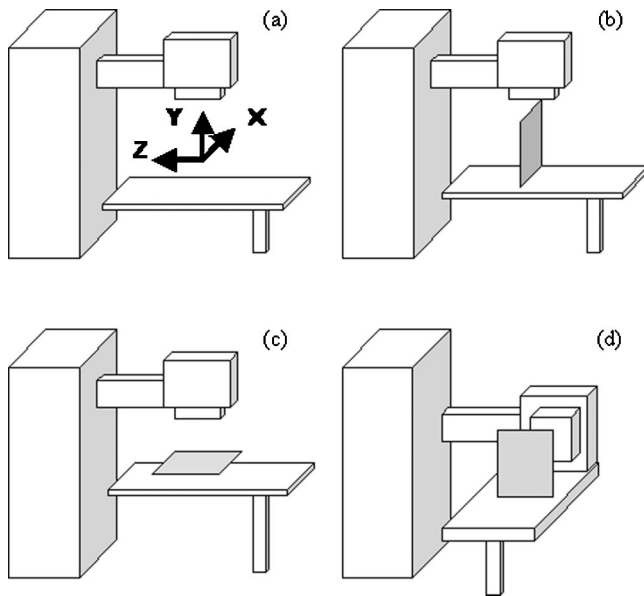
FIG. 1. xyz coordinate system with the z axis along the gantry rotation axis and the origin at the isocenter (a). Films are irradiated at different positions depending on the plane or axis of interest (b), (c) and (d).
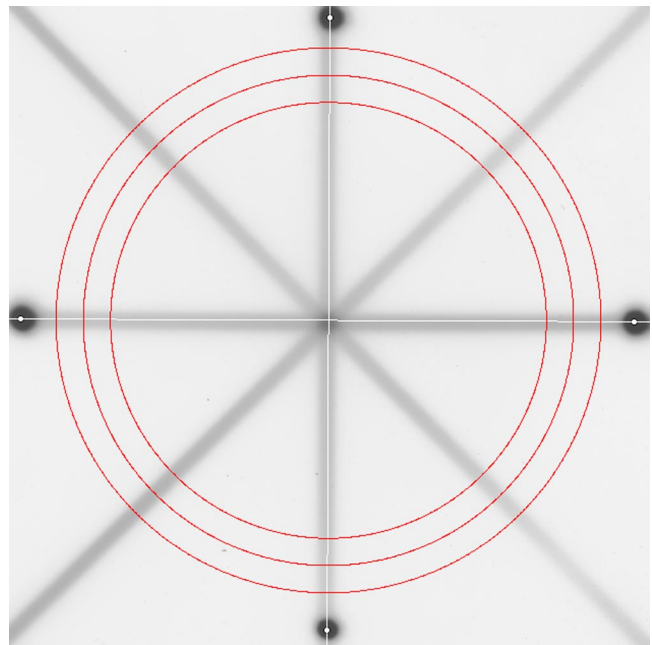

FIG. 2. The two-dimensional star-shot is analyzed by scanning the pixel value along three concentric circumferences. The center of the circumferences is obtained as the intersection of the laser lines marked on the film.

tion coefficient $\rho \geq 0.9993$). The pixel size used was of 250 μm.

In order to implement the procedure a software application was developed in Pascal using Delphi 6.0 (Borland Software Corporation, Scotts Valley, CA).

A. Isocenter films

Five films were used to determine the isocenter position and its size. Each film was placed in a plane perpendicular or parallel to one of the rotation axes in order to study the isocenter wobble in that particular plane or axial direction. The laser lines were marked on each film in order to establish a common spatial reference. The xyz coordinate system has been chosen with the z axis along the gantry rotation axis [Fig. 1(a)] and the origin has been taken at the isocenter.

Two films were irradiated to evaluate the isocenter wobble due to gantry rotation. The first film was placed in a plane perpendicular to the gantry axis [Fig. 1(b)] and was irradiated at gantry angles of 0, 90, 225 and 315°. The second film was placed horizontally on the table [Fig. 1(c)] and irradiated at gantry incidences of 0 and 180°. Two beams of collimator angles 0 and 90° were used for the vertically up irradiation of the film, and two beams of collimator angles 10 and 350° were used for the vertically down irradiation. In this way if the gantry sag in the axial direction due to gravity is the predominant contributor to the isocenter wobble, the diameter of the minimum circle intersecting the central rays of the beams will be close to the value of the sag.

An analogous procedure was applied to the couch rotation. The third film was placed on the table horizontally [Fig. 1(c)] and irradiated at couch angles of 0, 45, 90 and 315°, respectively. The fourth film was positioned vertically [Fig. 1(b)] and the lasers were marked. Then the couch was rotated to 90° [Fig. 1(d)] and the film was irradiated with two

beams of collimator angles 0 and 90°. After that, the couch was rotated to 270° and two beams of collimator 80 and 100° were used to irradiate the film.

The fifth film was used to determine the isocenter wobble due to collimator rotation. The film was placed horizontally on the table as shown in Fig. 1(c), in a plane perpendicular to the collimator rotation axis. The film was then irradiated with four beams of collimator angles 0, 90, 315 and 225°, respectively.

B. Two-dimensional (2-D) star-shots analysis

1. Central rays determination

Once the film has been processed and digitized, the star-shot image is loaded and represented on the computer screen. By clicking on the laser marks the laser intersection is calculated and is taken as the center of three concentric circumferences (Fig. 2). The radii of the circumferences are then chosen in such a way that all their points are away from the superposition area of the beams. The pixel value (PV) is sampled, using bilinear interpolation, along these circumferences with a step size of 0.18 degrees. Figure 3(a) plots the PV versus the angle Θ as read in this way. In order to reduce the high frequency noise, the curve is low pass filtered by circular convolution[13] with a Gaussian filter. After that, the mean value of the PV curve is subtracted from the curve, so that the new one has mean value of zero (Fig. 3(b)). Then zero crossing locations are detected by scanning for the positive-to-negative and negative-to-positive changes on the latter curve. On the star-shot image the points corresponding to zero crossings can be grouped in pairs, each pair representing two symmetrically located points on one beam profile. Their mid point will lie on the beam central ray. The
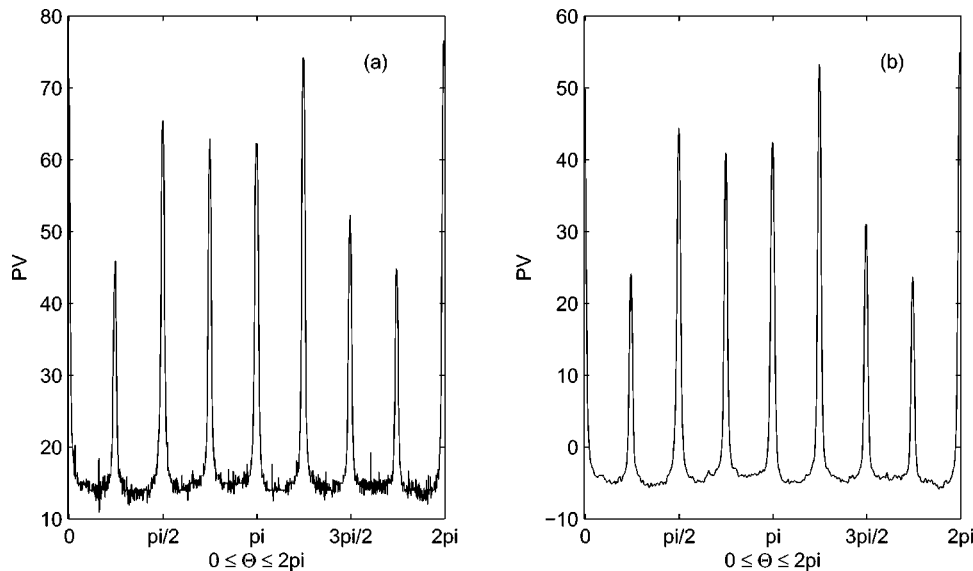
FIG. 3. The scan along one circumference results in a noisy curve (a). After its processing by low pass filtering and mean value subtraction a smoother one is obtained (b).

central rays of the beams are then obtained by fitting straight lines between their corresponding points (Fig. 4).

2. Minimum circle intersecting the central rays

The next step is to look for the smallest circle that intersects all of the central rays previously determined. First, the intersections $P_1, P_2, \ldots, P_n$ of every pair of rays are calculated. Then the median of the coordinates of the resulting points are the coordinates of a point taken as the origin for the search of the circle center. Centered on this point, for every point in a 201×201 array with a grid spacing of 1.00 pixels, the maximum distance to the axes is calculated. The point for which this maximum distance is smallest is taken as the origin for a new search with a grid spacing of 0.01 pixels. The resulting point is taken as the center of the minimum circle intersecting all the central rays in the plane of the star-shot under consideration, and its maximum distance to the axes is taken as the radius of the circle.

3. Accuracy and precision

In order to test the automated analysis implemented, six star-shots defining pentagon-like and triangle-like intersections (Fig. 5) were drawn and analyzed by the software. The star-shots were created by drawing intersecting beams. Each beam was defined by an axis (a straight line determined by a point and a direction), and by a transversal profile. The transversal profile of the beams was chosen to be Gaussian, and was characterized by its width w and amplitude a:

$$-a * \exp\left[-\left(\frac{d(i,j)}{w}\right)^2\right],$$

where $d(i,j)$ stands for the distance from the pixel with coordinates (i,j) to the beam axis. The star-shots images had a size of 400×400 pixels and were stored in BMP format. Their profile had an amplitude of one hundred gray scale levels and a width of seven pixels. The radii of the circles inscribed in the triangle or pentagon formed by the axes were

chosen to be of one, five and ten pixels. The software was tested by calculating the isocenter radius thirty times for each image. As a scan center, the known star-shot center position and twenty nine extra points were used. The scan radii chosen were 180, 160 and 140 pixels.

C. Determination of the 3-D radiation isocenter

The process of determining the central rays, described above, generates as output the equations for the central rays in the plane of the star-shot. As the star-shot planes in space are known, the 3-D spatial equation for the central rays can be readily obtained. Then, a procedure analogous to that used in the 2-D case is followed to determine the 3-D radiation
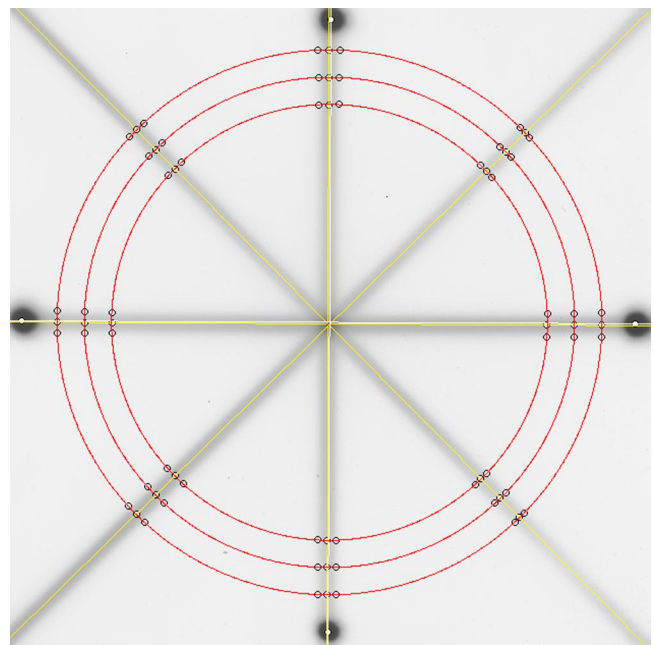

FIG. 4. Zero-crossing is used to determine points symmetrically located on the beam profiles. The central rays of the beams can be obtained by fitting straight lines between their midpoints.
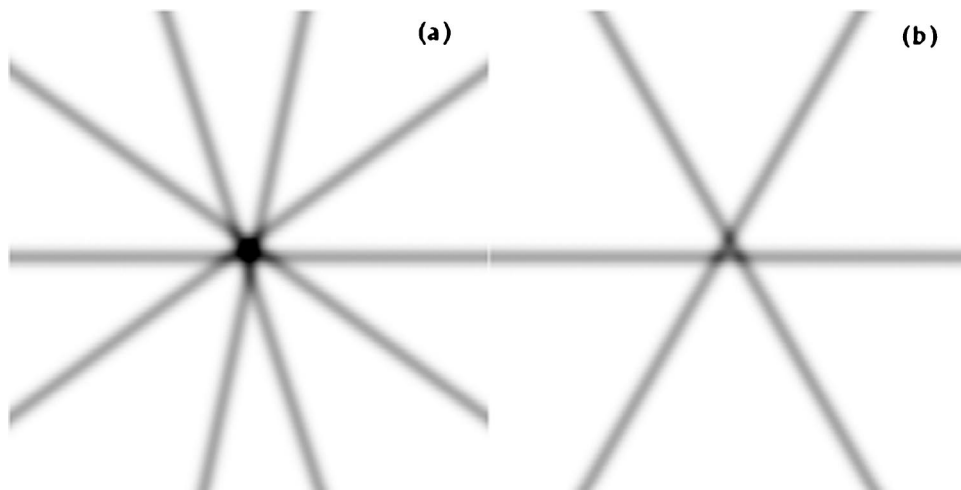
FIG. 5. Star-shots were drawn to evaluate the accuracy and precision of the software routines developed. Pentagon-like (a) and triangle-like (b) star-shots were used for this purpose.

isocenter. The maximum distance to the straight lines is calculated for every point in a $41 \times 41 \times 41$ array with a grid spacing of 1.00 pixels and centered in the laser intersection. The point for which this maximum distance is smallest is taken as the radiation isocenter position, and its maximum distance to the central rays is taken as the isocenter size.

III. RESULTS AND DISCUSSION

The accuracy and precision for the 2-D star-shot analysis presented was better than 1% of the pixel size in all the cases analyzed. Therefore the 2D automated analysis may substitute the traditional manual delineation of the central rays and
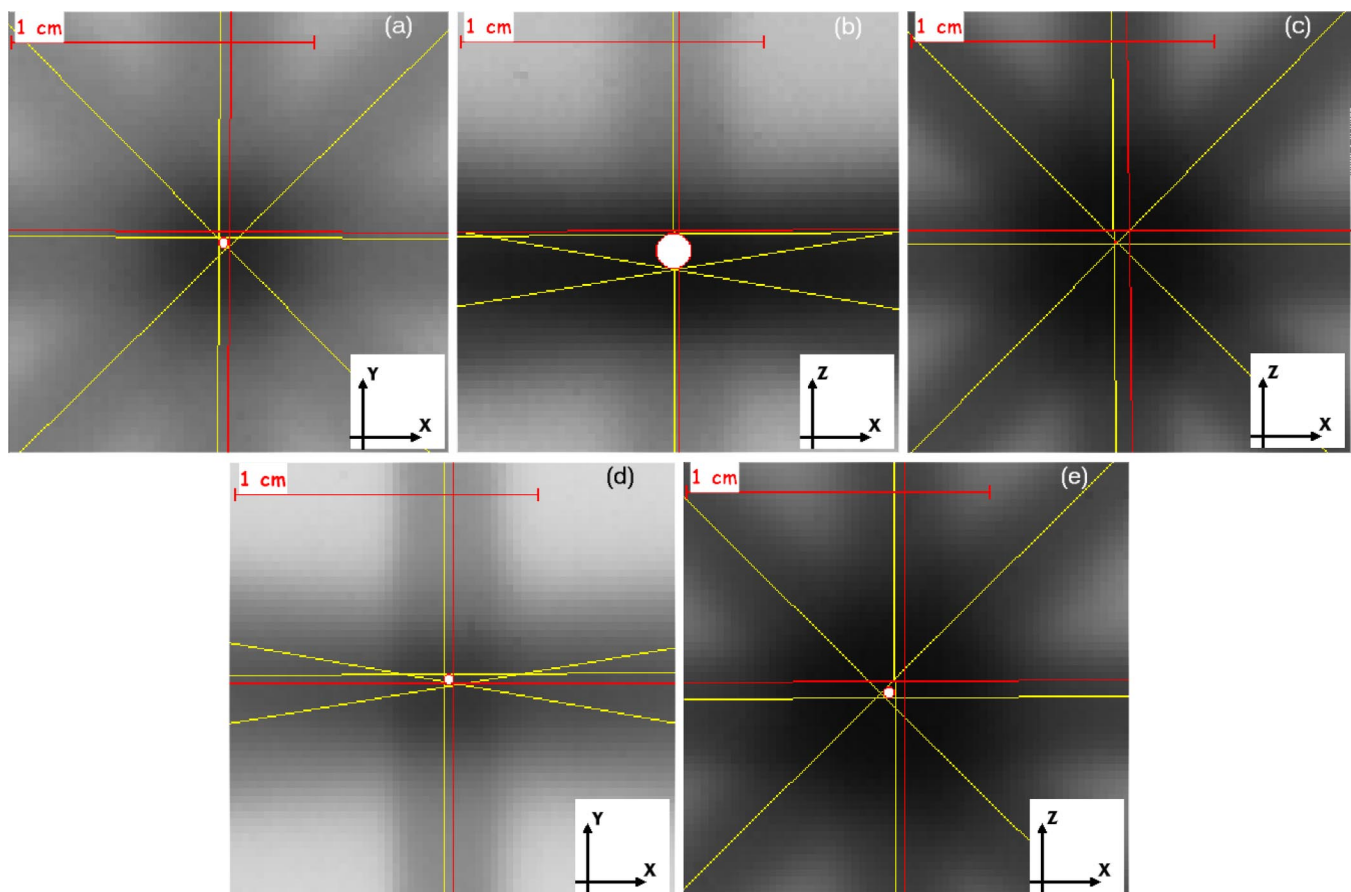

FIG. 6. Laser lines, central rays and the isocenter bounding circle for five star-shots employed in a radiation isocenter determination: Gantry star-shots in the xy plane (a) and xz plane (b), couch star-shots in the xz plane (c) and xy plane (d) and a collimator star-shot (e).

the isocenter bounding circle determination in such a way that the uncertainties associated with the analysis are minimal.

Figure 6 shows the analysis for a complete set of the five star-shot films. The red lines represent the laser lines, the yellow lines represent the central axes determined and the circle intersecting the axes is represented in white. It can be seen that the main contribution to the isocenter wobble for the accelerator studied occurs for the gantry rotation in the rotation axis direction.

The results for the measurement of the radiation isocenter position with respect to the laser intersection were -0.6 ± 0.2 mm in the x direction, -0.1 ± 0.3 mm in the y direction and -0.4 ± 0.3 mm in the z direction. The size of the radiation isocenter measured was of 1.0 mm ± 0.2 mm. All uncertainties are expressed as 2 standard deviations of the measurements.

[a] Electronic mail: afgonzalez@inicia.es

[1] R. Nath, P. J. Biggs, F. J. Bova, C. C. Ling, J. A. Purdy, J. van de Gein, and M. S. Weinhous, "AAPM code of practice for radiotherapy accelerators: Report of AAPM Radiation Therapy Task Group No. 45," Med. Phys. **21**, 1093–1121 (1994).

[2] G. J. Kutcher, L. Coia, M. Gillin, W. F. Hanson, S. Leibel, R. J. Morton, J. R. Palta, J. A. Purdy, L. E. Reinstein, G. K. Svenson, M. Weller, and L. Wingfield, "Comprehensive QA for radiation oncology: Report of AAPM Radiation Therapy Commitee Task Group 40," Med. Phys. **21**, 581–618 (1994).

[3] A. L. Boyer, "Quality assurance foundations in equipment specification, acceptance testing and commissioning," in *Quality Assurance in Radiotherapy Physics*, edited by G. Starkschall and J. Horton (Medical Physics Publishing, Madison, WI, 1991), pp. 5–21.

[4] AAPM Task Group 10, "Code of Practice for x-ray therapy linear accelerators," Med. Phys. **2**, 110–121 (1975).

[5] F. R. Hudson, "A simple isocenter checking procedure for radiotherapy treatment machines using the optical pointer," Med. Phys. **15**, 72–73 (1988).

[6] M. K. Woo, "A personal-computer-based method to obtain "star-shots" of mechanical and optical isocenters for gantry rotation of linear accelerators," Med. Phys. **29**, 2753–2755 (2002).

[7] M. K. Woo, P. O'Brien, B. Gillies, and R. Etheridge, "Mechanical and radiation isocenter coincidence: An experience in linear accelerator alignment," Med. Phys. **19**, 357–359 (1992).

[8] F. A. Gibbs, Jr., D. Buechler, D. D. Leavitt, and J. H. Moeller, "Measurement of mechanical accuracy of isocenter in conventional linear-accelerator-based radiosurgery," Int. J. Radiat. Oncol., Biol., Phys. **25**, 117–122 (1992).

[9] J. San Tsai, B. H. Curran, E. S. Sternick, and M. J. Engler, "The measurement of linear accelerator isocenter motion using a three-micrometer device and an adjustable pointer," Int. J. Radiat. Oncol., Biol., Phys. **34**, 189–195 (1996).

[10] W. R. Lutz, *Proceedings of the Symposium on Quality Assurance of Radiotherapy Equipment*, in AAPM Symposium Proceedings 3, Kansas City, MO (American Institute of Physics, Woodbury, NY, 1982), pp. 50–73.

[11] B. Arjomandy and M. D. Altschuler, "A quality assurance device for the accuracy of the isocentres of teletherapy and simulation machines," Phys. Med. Biol. **45**, 2207–2217 (2000).

[12] T. Falco, M. Lachaine, B. Poffenbarger, E. B. Podgorsak, and B. G. Fallone, "Setup verification in linac-based radiosurgery," Med. Phys. **26**, 1972–1978 (1999).

[13] A. K. Jain, *Fundamentals of Digital Image Processing* (Prentice–Hall, Englewood Cliffs, NJ, 1989), Vol. 1, Chap. 5, p. 144.